On Computing Power System Steady-State Stability Using Synchrophasor Data

Karl E. Reinhard
Dept of Electrical & Computer Engr
Univ of Illinois at Urbana-Champaign
reinhrd2@illinois.edu

Peter W. Sauer
Dept of Electrical and Computer Engr
Univ of Illinois at Urbana-Champaign
sauer@illinois.edu

Alejandro D. Domínguez-García
Dept of Electrical & Computer Engr
Univ of Illinois at Urbana-Champaign
aledan@illinois.edu

***Abstract*—In electric power systems, a key challenge is to quickly and accurately estimate how close the system is to its stability limits. This paper investigates using synchrophasor measurements at two buses connected by a transmission line to calculate parameters for a pair of Thevenin equivalent sources, which when connected by the transmission line model provide an equivalent power system representation. As seen from the transmission line, the angle difference between the two Thevenin equivalent sources is termed the "angle across the system" for that transmission line. In the case of a lossless transmission line with voltage support on both ends, the "angle across the system" (as seen from the line) is the difference between the transmission line bus voltage phase angles; to ensure steady-state stability under these conditions, it is well known that this angle difference must be less than 90 degrees. This paper extends these ideas and proposes the notion of the "angle across the system" described above as a gauge for assessing the system's proximity to its stability limit.**

I. Introduction

Electric power systems have well documented transmission line power transfer capacity limits. A continuing challenge is real-time operator awareness of the power system's state versus known operating limits. Today, the power system's state is estimated several times per hour, which guides power system operators to continually balance power and generation to maintain very reliable, stable system operation. Meeting these high expectations requires conservative power system operation to protect against uncertainties and unexpected system conditions, which might lead to power system loadability violations. The Smart Grid initiative is bringing a synchrophasor data network on-line that will provide near real-time, precisely synchronized bus voltage, current, and power measurements that provide an opportunity to advance from operating the power system with estimates to measurements.

This paper investigates using synchrophasor measurements from two buses to compute model parameters for a pair of Thevenin sources, which with the connecting transmission line parameters enable a two-bus equivalent power system representation. The difference between the resulting Thevenin equivalent source angles is proposed as an indicator of how close the system is to its stability limits. The largest Thevenin equivalent source angle difference among the connected bus pairs in the system becomes a measure indicating the risk of losing system stability. This offers the possibility of a simple, near-real time system stability assessment measure without the requirement for system-wide state measurements, complex system models, and powerful computer systems to compute existing risk measures.

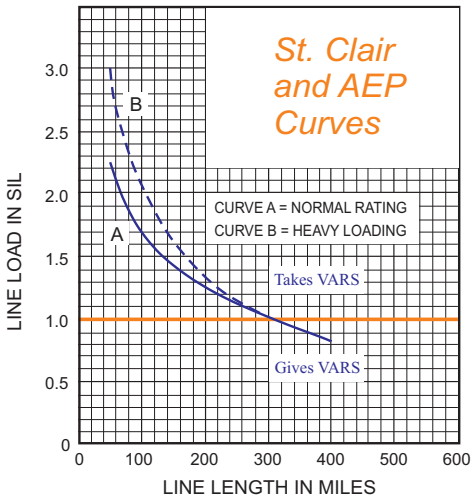

Fig. 1: St. Clair and AEP Curves [1], [2].

II. Preliminaries

There are many factors that restrict power system operations. Among them are the thermal, voltage, and stability transmission line limitations. Short lines are thermally limited; medium length lines are voltage drop limited; and long lines are stability limited. Harry P. St. Clair provided empirical line loadability limits in what have become known in the power industry as the St. Clair Curves [1]. These loadability limit notions are rooted in well understood phenomena. Thermal and voltage constraints are set by line currents and bus voltages respectively – both easily measured. The stability constraint related to phase angle differences is more difficult to measure; the constraint is simply illustrated in the relationship for real power flow from bus 1 to bus 2 on a lossless line with voltage support on both ends, which is given by

$$P_{12} = \frac{V_1 V_2}{X_{12}} \sin\left(\delta_1 - \delta_2\right), \tag{1}$$

where, X_{12} is the line series reactance and $V_1\angle\delta_1$ and $V_2\angle\delta_2$ are the respective bus voltage magnitudes and phase angles. Maximum power flow is reached when the voltage phase

angle difference, $\delta_1 - \delta_2$, between the buses reaches 90 degrees; beyond this angle difference, it is well known that the system is no longer steady-state stable. The authors in [2] validated and extended St Clair line loadability limits to extra-high voltage lines using numerical techniques – providing the St. Clair curves shown in Fig. 1. This paper uses a π equivalent transmission line with Thevenin equivalent models on the sending and receiving ends; it also used 45 degrees as the stability margin limit. A similar approach for detecting loadability constraints is proposed in [3]. The authors in [4] and [5] propose using local current and voltage measurements to compute Thevenin equivalent circuits.

The St. Clair curves and the application of Thevenin equivalent models form the basis for the ideas advanced in this paper. Consequently, we envision that our Thevenin equivalent application will retain the notions of thermal, voltage-drop, and stability constraints. Whereas Thevenin equivalents have previously been used to determine line loadability limits, this paper proposes using equivalents to gauge closeness to loadability limits. Our goal is to compute a real-time "angle across the system" (AnglxSys) for each line using Thevenin equivalents. These equivalents are obtained from synchrophasor measurements. Our conjecture is that when the power system is nearing its loadability limit, the AnglxSys for at least one line will be approaching 90 degrees. In this paper, the analysis and results focus on the methods and feasibility of computing the AnglxSys for a given line using actual synchrophasor data.

III. Estimating Thevenin Equivalents From Synchrophasor Data

Per our conjecture, the AnglxSys as seen from two buses connected to opposing ends of a transmission line is a pre-eminent indicator of the system's proximity to its steady-state stability limit – the most difficult to determine of the three stability indicators listed above. Our objective is to develop a Thevenin equivalent circuit representation composed of an equivalent voltage source (voltage magnitude and angle) and impedance, which characterizes the power system's behavior as seen from the end of a particular transmission line. The boxed portion of the circuit in Fig. 2 represents such a Thevenin equivalent of the power system looking into bus 1. The transmission line connecting buses 1 and 2 is modeled by the known line impedance, $R_l + jX_l$. A second Thevenin equivalent representing the power system behind the terminals at bus 2 completes the proposed circuit. In this model, we have neglected the shunt elements.

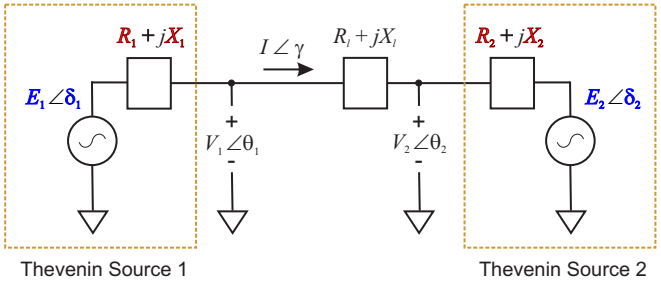

Fig. 2: Thevenin Equivalent Circuit Model.

The challenge is to develop a reliable, accurate method for determining Thevenin equivalent circuit parameters from field measurements. In particular, we propose using synchrophasor data measured by phasor measurement units (PMUs) at two connected bus terminals of interest to compute two Thevenin equivalent circuits. The proposed Thevenin equivalent stability indicator (the difference between the Thevenin source angles) could be easily computed from PMU measurements. This would allow power system operators to continuously monitor the AnglxSys and use it to gauge closeness to unstable conditions.

The common method for finding a Thevenin equivalent circuit is to measure the open circuit voltage, V_{oc}, and to measure the short circuit current, I_{sc}, across the terminal pair. These voltage and current values determine the axis crossings; the slope of the line connecting the two axis crossings is the Thevenin equivalent impedance; Fig. 3 shows a Thevenin equivalent circuit characteristic for a purely resistive circuit. A Thevenin equivalent circuit with the inductive and capacitive elements needed to model an AC electric power system would add two more dimensions to span the solution space. Unfortunately in practice, it is impossible to obtain V_{oc} and I_{sc} while the line is in operation. Assuming the power system $I - V$ relationship is nearly linear in the anticipated operating range, a Thevenin equivalent (green line) could be determined by measurements. Determining the equivalent circuit is complicated by noise in PMU voltage and current measurements; which conceptually will result in a range of Thevenin equivalent parameter extremes as indicated by the dashed orange lines crossing the respective axes. This prompts the caveat that poorly conditioned data may result in large equivalent parameter value swings between data sets collected under nearly identical operating conditions.

Consider the Thevenin source 1 circuit in Fig. 2; in order to simplify the notation in subsequent developments, the sub-index 1 is dropped from all the variables. The relation between the variables is described by the complex equation

$$E\angle\delta = I\angle\gamma \cdot (R + jX) + V\angle\theta. \tag{2}$$

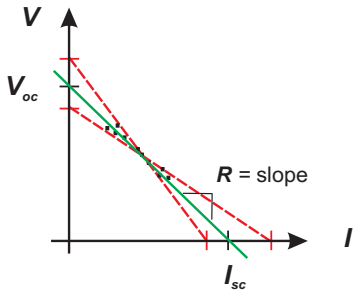

Fig. 3: Thevenin Equivalent I-V Characteristic (resistance only).

Time (s)	V_1 (KV)	θ_1 °	$P_{1->2}$ MW at Bus 2	$Q_{1->2}$ MVAR at Bus 2	V_2 (KV)	θ_2°
0.00	759.26	62.286	2409.4	-542.98	762.76	60.724
0.10	759.27	62.405	2409.4	-542.98	762.77	60.841
0.20	759.27	62.524	2409.4	-542.98	762.76	60.963
0.30	759.33	62.642	2409.4	-542.98	762.77	61.079
0.40	759.31	62.758	2409.4	-542.98	762.76	61.193
0.50	759.26	62.876	2409.4	-542.98	762.73	61.312
0.60	759.23	62.989	2409.4	-542.98	762.68	61.427
0.70	759.18	63.107	2409.4	-542.98	762.64	61.543
0.80	759.18	63.223	2409.4	-542.98	762.66	61.66
0.90	759.21	63.343	2409.4	-542.98	762.65	61.779
1.00	759.19	63.456	2409.4	-542.98	762.65	61.892
1.10	759.2	63.572	2409.4	-542.98	762.65	62.011
1.20	759.19	63.685	2409.4	-542.98	762.63	62.121
1.30	759.16	63.803	2409.4	-542.98	762.63	62.24
1.40	759.15	63.916	2409.4	-542.98	762.61	62.356
1.50	759.13	64.035	2409.4	-542.98	762.63	62.47
1.60	759.16	64.151	2409.4	-542.98	762.61	62.585
1.70	759.16	64.264	2409.4	-542.98	762.64	62.699
1.80	759.19	64.38	2409.4	-542.98	762.63	62.814
1.90	759.18	64.498	2409.4	-542.98	762.62	62.93
2.00	759.16	64.726	2409.4	-542.98	762.65	63.159

TABLE I: Sample Synchrophasor Data.

By writing the complex variables in Cartesian form, i.e. $E\angle\delta = E_r + jE_i$, $I\angle\gamma = I_r + jI_i$, and $V\angle\theta = V_r + jV_i$, we obtain an equivalent pair of equations:

$$E_r = R\,I_r - X\,I_i + V_r \tag{3}$$
$$E_i = X\,I_r - R\,I_i + V_i. \tag{4}$$

Note that in (2) and its equivalent pair (3) and (4), there are 4 unknown variables: real and imaginary Thevenin source terms, E_r and E_i and unknown constitutive impedance, consisting of resistance R and reactance X. There are multiple approaches to solving the Thevenin equivalent problem: i) to use a set of 2 sequential PMU measurements to enable an exact solution, ii) to use 3 or more sequential measurements to find a least squares error (LSE), and iii) to reduce the number of unknowns by fixing one or more of the four unknown values.

The exact solution requires 2 consecutive measurement sets, which results in 4 equations and 4 unknowns. This equation set can be in matrix form as

$$\begin{bmatrix} 1 & 0 & -I_{r_{(1)}} & I_{i_{(1)}} \\ 0 & 1 & -I_{i_{(1)}} & -I_{r_{(1)}} \\ 1 & 0 & -I_{r_{(2)}} & I_{i_{(2)}} \\ 0 & 1 & -I_{i_{(2)}} & -I_{r_{(2)}} \end{bmatrix} \begin{bmatrix} E_r \\ E_i \\ R \\ X \end{bmatrix} = \begin{bmatrix} V_{r_{(1)}} \\ V_{i_{(1)}} \\ V_{r_{(2)}} \\ V_{i_{(2)}} \end{bmatrix}, \tag{5}$$

with the first and second data measurement sets indicated in parentheses. From a purely mathematical standpoint, this would appear to solve the problem provided that the left-hand matrix is invertible – which depends upon measured data characteristics.

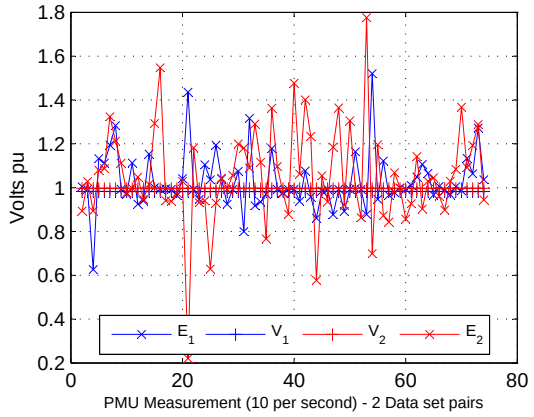

(a) Numerical Thevenin source magnitudes.

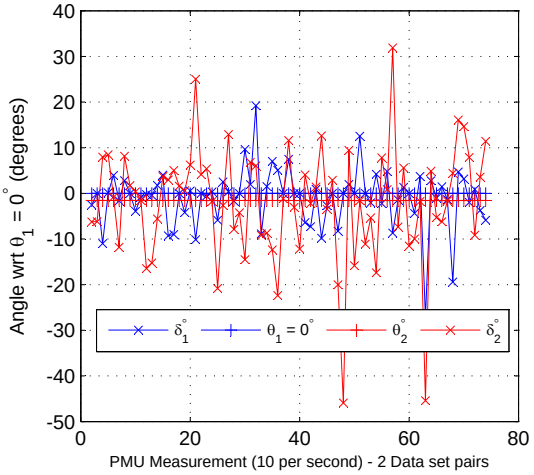

(b) Numerical Thevenin source phase angles.

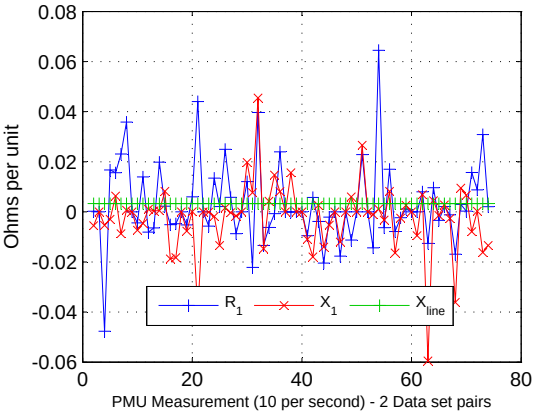

(c) Numerical Results – Source 1 Thevenin resistance and reactance.

Fig. 4: Exact Thevenin Source Solutions

A. *Numerical Results*

Table I shows a typical synchrophasor data set for a 765KV transmission line that includes line-to-line voltage magnitude and phase angle. Power is flowing from bus 1 to bus 2. As is typical of a power system, the measured frequency varies just under 0.02 Hz from the nominal 60 Hz system frequency,

$$A^{-1} = \begin{bmatrix} 1+\frac{-b\,(a-c)+a[(b-d)-(a-c)\,f]}{(a-c)^2} & \frac{b}{(b-d)\,f}-\frac{a}{(a-c)\,f} & \frac{b\,(a-c)+a[(d-b)+(a-c)\,f]}{(a-c)^2 f} & -\frac{b}{(b-d)\,f}+\frac{a}{(a-c)\,f} \\ \frac{a\,(a-c)+b[(b-d)-(a-c)\,f]}{(a-c)^2 f} & 1-\frac{a}{(b-d)\,f}-\frac{b}{(a-c)\,f} & \frac{-a\,(a-c)+b[(a-c)\,f-(b-d)]}{(a-c)^2 f} & \frac{a}{(b-d)\,f}+\frac{b}{(a-c)\,f} \\ \frac{(b-d)-(a-c)\,f}{(a-c)^2 f} & \frac{-1}{(a-c)\,f} & \frac{(a-c)\,f-(b-d)}{(a-c)^2 f} & \frac{1}{(a-c)\,f} \\ \frac{1}{(a-c)\,f} & \frac{-1}{(b-d)\,f} & \frac{-1}{(a-c)\,f} & \frac{1}{(b-d)\,f} \end{bmatrix}, \quad (6.1)$$

$$\text{where} \qquad f = \frac{(a-c)^2+(b-d)^2}{(a-c)(b-d)}$$

which accounts for the voltage angles' slow rotation. The real and reactive power flows allow calculation of current magnitude and angle. For calculations, the sample data was normalized and converted to per phase, per unit data for calculations. Typically, the data values over short time periods showed only small changes. For example, the per unit voltage measurement mean over 2400 measurements (10 measurements per second) was 1.0003 with variance $7.062 \cdot 10^{-8}$ $\mathrm{V_{pu}}$. The per unit currents measurement calculated from the data showed similar stability with mean .9587 and variance $1.251 \cdot 10^{-5}\mathrm{A_{pu}}$.

We applied the exact solution approach to the data outlined above. The calculated Thevenin source magnitudes, phase angles, and impedances are shown respectively in Figs. 4a, 4b, and 4c. The computed Thevenin source parameter values were striking in their wildly erratic swings; swings that run counter to intuition and call into question their value for modeling system behavior. For instance, the Thevenin source magnitudes are expected to be close to 1.0 per unit and certainly to not swing across a range exceeding 1.0 V_{pu}. Similarly, the phase angle relationships are not consistent with power flow from source 1 to source 2, i.e. that the voltage phase angles be characterized by $\delta_1 > \theta_1 > \theta_2 > \delta_2$. Finally, the impedance values not only rapidly swing, but also improbably take on negative values, which is difficult to accept or justify. As outlined in the next section, we found that the erratic Thevenin parameter behavior was attributable to sample synchrophasor data characteristics.

B. Matrix Condition Numbers

1) 2 measurement pairs: Consider the matrix on the left-hand side of (5) :

$$\begin{aligned} A &= \begin{bmatrix} 1 & 0 & -I_{r_{(1)}} & I_{i_{(1)}} \\ 0 & 1 & -I_{i_{(1)}} & -I_{r_{(1)}} \\ 1 & 0 & -I_{r_{(2)}} & I_{i_{(2)}} \\ 0 & 1 & -I_{i_{(2)}} & -I_{r_{(2)}} \end{bmatrix} \\ &= \begin{bmatrix} 1 & 0 & -a & b \\ 0 & 1 & -b & -a \\ 1 & 0 & -c & d \\ 0 & 1 & -d & -c \end{bmatrix}, \end{aligned} \quad (6)$$

with the inverse of A as given in (6.1). The condition number of A is an important measure of the sensitivity of the solution

$$x = [\, E_r \;\; E_i \;\; R \;\; X \,]^T \quad (7)$$

to small perturbations in the measurement vector

$$b = \left[\, V_{r_{(1)}} \;\; V_{r_{(1)}} \;\; V_{r_{(2)}} \;\; V_{i_{(2)}} \,\right]^T \quad (8)$$

The condition number is defined for the norm p as

$$K(A) = \|A\|_p \left\|A^{-1}\right\|_p . \quad (9)$$

The L_1 ($p = 1$, maximum absolute column sum) and L_∞ ($p = \infty$, maximum absolute row sum) norms are easily computed to provide accurate condition number order of magnitude estimates. A desirable matrix condition number is close to one; in which case, small measurement errors have negligible impact upon the solution. In contrast, a very large matrix condition number amplifies small measurement errors to substantially affect the computed solution. Using the synchrophasor data in Table I, the L_1 and L_∞ norms of A^{-1} are easily estimated. The differences between sequential real and imaginary current measurements are both very small, such that

$$\left(I_{i_{(1)}} - I_{i_{(2)}}\right) = (b-d) \sim 10^{-3} \quad (10)$$

$$\left(I_{i_{(1)}} - I_{i_{(2)}}\right) = (b-d) \sim 10^{-3} \quad (11)$$

$$f = \frac{(a-c)^2+(b-d)^2}{(a-c)(b-d)} \sim \frac{(10^{-3})^2+(10^{-3})^2}{(10^{-3})(10^{-3})} \sim 1 \,, \quad (12)$$

which results in $\|A\|_1 \sim \|A\|_\infty \sim 1$ and $\left\|A^{-1}\right\|_1 \sim \left\|A^{-1}\right\|_\infty \sim 10^3$. The resulting condition numbers are much greater than the ideal condition number that is close to 1, in particular:

$$K(A) = \|A\|_p \left\|A^{-1}\right\|_p \sim 10^3 \,. \quad (13)$$

The consequence of the condition number being on the order of 10^3 is that small perturbations in b may disproportionally change the calculated solution – casting doubt on the accuracy of computed results. We found that the sample data matrices had condition numbers on the order of 10^5 – as shown in Fig. 5. The impact of these extremely large condition numbers is evident in the dramatic Thevenin parameter swings in Figs 4a, 4b, and 4c.

2) More than 2 measurement pairs: We also considered using an LSE solution to reduce the Thevenin parameter swings. The LSE solution incorporates additional data pairs – generating a rectangular $m \,\mathrm{x}\, n$ matrix with $m > n$. The condition number can be computed using the ratio of the

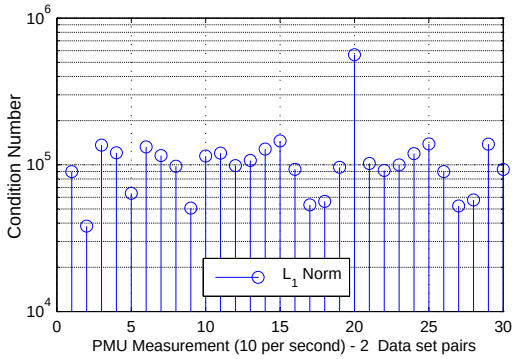

Fig. 5: Sample condition numbers for 30 consecutive Thevenin parameter sets.

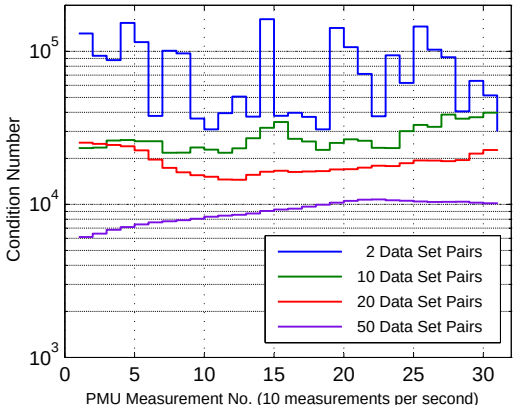

Fig. 6: Least squares error estimate condition numbers computed using 2, 10, 20, and 50 data set pairs.

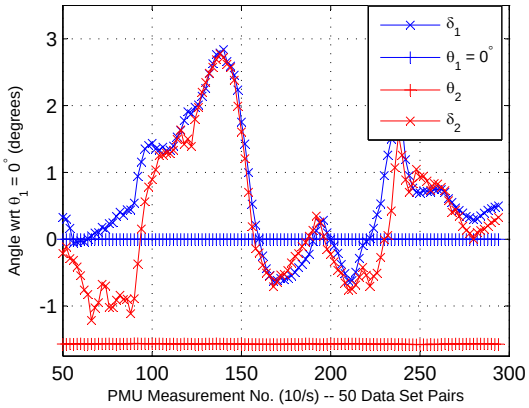

Fig. 7: Over determined Thevenin source phase angles.

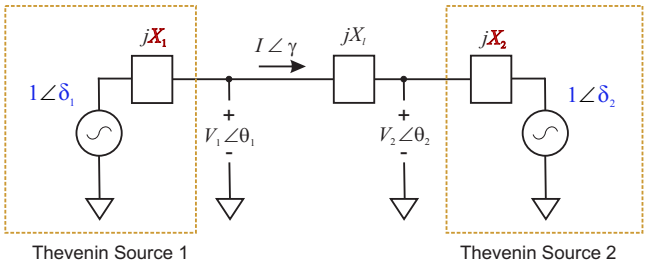

Fig. 8: Simplified Thevenin equivalent model.

largest to smallest of the ordered singular values, σ_i, obtained from the singular value decomposition of the matrix A. The condition number is

$$K(A) = \frac{\sigma_1}{\sigma_n}, \quad \sigma_1 > \ldots > \sigma_i > \ldots > \sigma_n. \tag{14}$$

Unlike the fully determined system in (6), a straight forward estimate of the overdetermined system's condition number is very difficult to derive. To determine whether the LSE solution improved the problem's conditioning, we used MATLAB to compute condition numbers for over determined matrices constructed from 10, 20, and 50 sample data set pairs. The results in Fig. 6 clearly show that the condition number does not appreciably improve even using 50 data set pairs. Further, Fig. 7 shows that while the Thevenin source phases do not swing erratically, they also do not satisfy the fundamental condition $\delta_1 > \theta_1 > \theta_2 > \delta_2$ that is characteristic of power flowing from source 1 to source 2.

C. Simplified Thevenin Equivalent Model

Figure 8 shows an alternative Thevenin equivalent model. In this model, we fix the source magnitudes $|E_1| = |E_2|$ to 1 p.u. and specify that the Thevenin equivalent impedances be purely reactive, i.e. $R_1 = R_2 = 0$. Note that this circuit model carries forward the assumption that current flows through shunt capacitances are negligible; consequently, the two Thevenin source terminals share the same current. The Thevenin source 1 reactance, X_1, is determined by

$$1\angle\delta_1 = I\angle\gamma \cdot (jX_1) + V_1\angle\theta_1. \tag{15}$$

Decomposing (15) into its real and imaginary equations, the δ_1 term can be eliminated using the trigonometric identity

$$\sin\,\delta_1 = \sqrt{1 - \cos^2\delta_1}, \tag{16}$$

which results in the quadratic equation

$$I^2X_1^2 - 2V_1I\,\sin\,(\gamma)\,X_1 - (V_1^2 - (1)^2) = 0, \tag{17}$$

with two possible solutions

$$X_1 = \frac{1}{I}\left[V_1\sin\,(\gamma - \theta_1) \pm \sqrt{(1)^2 - V_1^2\cos^2(\gamma - \theta_1)}\right]. \tag{18}$$

Similarly, we determine Thevenin source 2 reactance, X_2,

$$V_2\angle\theta_2 = I\angle\gamma \cdot (jX_1) + 1\angle\delta_2\ , \tag{19}$$

which yields two possible X_2 solutions of very similar form

$$X_2 = \frac{1}{I}\left[-V_2\sin(\gamma-\theta_2) \pm \sqrt{(1)^2 - V_2^2\cos^2(\gamma-\theta_2)}\right]\ . \tag{20}$$

The Thevenin source angles are determined by writing the system power balance equation

$$1\angle\delta_1\,(I\angle\gamma)^* = j(X_1+X_l+X_2)\,I^2 + 1\angle\delta_2\cdot(I\angle\gamma)^*\ . \tag{21}$$

The real power equation reduces to $\cos(\delta_1-\gamma) = \cos(\delta_2-\gamma)$, which is satisfied if $\delta_1 = \delta_2$ (a trivial solution with no power flow); alternatively since $\cos(\alpha) = \cos(-\alpha)$,

$$\delta_2 = 2\gamma - \delta_1 \ \equiv\ \gamma = \frac{\delta_1+\delta_2}{2} \tag{22}$$

is also a solution. Using these relationships, we obtain

$$\delta_1 = \gamma + \sin^{-1}\left(\frac{(X_1+X_l+X_2)\,I}{2}\right) \tag{23}$$

$$\delta_2 = \gamma - \sin^{-1}\left(\frac{(X_1+X_l+X_2)\,I}{2}\right) \tag{24}$$

To compensate for the slow rotation of the phasor measurements due to the slight difference between the actual system frequency and the ideal 60 Hz frequency, the voltage angle at bus 1 is set to 0 (i.e. $\theta_1^{'} = 0 = \theta_1 - \theta_1$) and all other angles are adjusted by subtracting θ_1.

The effectiveness of these relationships was tested using the data set from which Table I is extracted. The resulting Thevenin source angle values and computed reactances are shown in Table II. Note that the X_1 and X_2 solutions are each composed of a pair of positive and negative reactance values; also, the four possible solutions show interesting symmetries. We confirmed that these solutions provided near-zero KVL residuals around each source loop and around the system loop; however, only the two positive reactance solutions resulted in the expected power flows based upon the relative phase angle relationships of the source and terminal voltages, i.e. $\delta_1 > \theta_1 > \theta_2 > \delta_2$. In the other three X_1 and X_2 solution combinations, the phase angle order is violated. The phase angle relations for the positive $X_1$and X_2 solutions are shown in Fig. 9.

This model was consistent with expected system behavior in every respect. The solution satisfied three KVL loop equations with small residuals – one through each source and its corresponding terminals and a loop around the total system. Additionally, the real and reactive powers computed at each source and terminal were consistent with expected real and reactive power flows. Further, the Thevenin equivalent solution showed results that varied no more quickly than the phasor measurements. Consequently, this model and Thevenin equivalent computational approach warrant further investigation for applications assessing power system stability.

δ_1^o	X_1	X_l	X_2	X_{total}	δ_2^o
-2.179	-.0043	.0034	-.0546	-.0555	24.37
10.95	.0506	.0034	-.0546	-.0006	11.25
11.22	-.0043	.0034	.0016	.0007	10.96
24.35	.0506	.0034	.0016	.0556	-2.161

TABLE II: Computed Thevenin Source Parameters*, $\gamma = 11.1^o$.
*Thevenin source values at $t = 1s$ averaging 10 PMU measurements. Angles and reactance are in degrees and ohms per unit respectively.

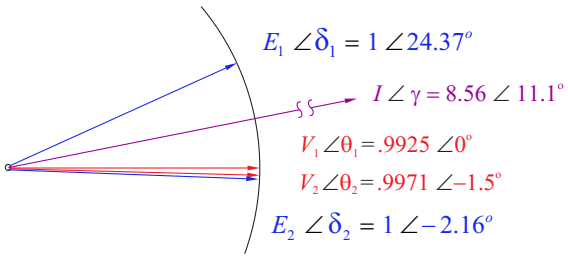

(a) Thevenin source values at $t = 1$ s averaging 10 synchrophasor measurements.

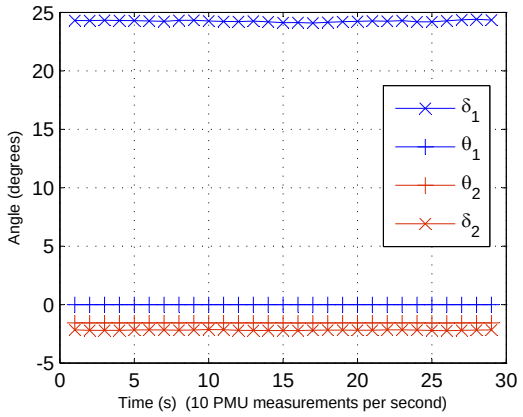

(b) Voltage phase angles using sets of 10 averaged synchrophasor measurements

Fig. 9: Thevenin source phase angle results using the positive X_1 and X_2 solutions, $\gamma = 11.1^o$.

IV. Conclusion

The determination of Thevenin Equivalent networks using Synchrophasor data is important for reducing the size of the interconnected network to the simplest possible level. These equivalents are useful for evaluating the health of the power system in real time. They provide a mechanism for assessing the closeness of the system to reliability limits without relying on a detailed mathematical model of the network and grid topology. This paper provided a discussion of the challenges associated with creating these Thevenin system equivalents – and identified a simplified Thevenin equivalent model that shows promise. Future work will investigate the utility of the proposed "angle across the line" measure of closeness to steady-state stability loadability limits.

REFERENCES

[1] H. P. St. Clair. Practical concepts in capability and performance of transmission lines. *Part III Power Apparatus and Systems Transactions of the American Institute of Electrical Engineers*, 72(2):1152–1157, 1953.

[2] R. Gutman, P. Marchenko, and R. D. Dunlop. Analytical development of loadability characteristics for ehv and uhv transmission lines. (2):606–617, 1979.

[3] T. He, S. Kolluri, S. Mandal, F. Galvan, and P. Rastgoufard. *Applied Mathematics for Restructured Electric Power Systems: Optimization, Control, and Computational Intelligence*, chapter Identification of Weak Locations in Bulk Transmission Systems Using Voltage Stability Margin Index, pages 25–37. Springer Science +Business Media, Inc., 2005.

[4] K. Vu, M. M. Begovic, D. Novosel, and M. M. Saha. Use of local measurements to estimate voltage-stability margin. 14(3):1029–1035, 1999.

[5] P. Zhang, L. Min, and N. Zhang. Method for voltage stability load shedding using local measurements, Oct 2009.

ACKNOWLEDGMENT

This work has been funded in part by the Consortium for Electric Reliability Technology Solutions (CERTS).